ICAS 2021 SHANGHAI
International Council of the Aeronautical Sciences
32nd Congress of the International Council of the Aeronautical Sciences
September 6-10, 2021 Pudong Shangri-La, Shanghai, China

ASSEMBLY QUALITY OPTIMIZATION APPROACH FOR LARGE-SCALE ACTIVE COMPONENTS BASED ON REVERSE ENGINEERING

Zhu Xusheng[1], Wang Haoyu[1], Liu Lei[1]

[1] AVIC Chengdu Aircraft Industrial (Group) Co., Ltd, Chengdu, 610091, China

Abstract

Compared with civil aircraft, assembly problems such as stepped difference, gap and interference will lead to more significant influence on aerodynamic and stealth performance. Advanced military aircrafts have stricter requirements than civil ones in large-scale active components assembly quality, because of stealth and supersonic demands. Aiming to improve assembly quality of large-scale active components, this paper proposes an optimization approach based on reverse engineering. Firstly, a main landing gear door is taken as example to illustrate inducements of active components assembly quality problem. Assembly error mainly source from the fabrication and assembly error of components and jigs. Because gap and interference in assembly process can be effectively solved by using conceal edge band, stepped difference is emphasized in this paper. Then, reverse engineering based on laser scanner is introduced. It is an efficient and accurate method to acquire measurement data and establish an existing model. Based on measurement data obtained by laser scanner, assembly quality optimization model based on measurement data is proposed. This model can compute the intersection hole axis of component which can effectively minimizing the assembly stepped difference. Drilling the intersection holes based on the computation result can significantly improve the assembly quality. The proposed mathematical model and method are verified through an experiment of main landing gear door simulator assembly. The example of measurement scenario demonstrates that the proposed method is feasible and effective and will lay a foundation for active component assembly quality improvement.

Keywords: assembly quality; reverse engineering; stepped difference; measurement

1. Introduction

Assemble process is the most important and time-consuming part in aircraft manufacturing and has significant impact on the aerodynamic performance of aircraft [1]. The mode of part-to-part assembly which aims to obtain interchangeability by improving machining or subassembly accuracy, is usually uneconomical and infeasible for large scale components of aircraft because of maintaining very close tolerance requirements over large structures and the large number of different operations for relatively low production volumes is difficult even impossible in aircraft assembly [1][2]. With regard to large-scale components in aircraft manufacturing industry, such as fuselages, wings, vertical/ horizontal tail, etc., the practical way is to persevere allowance on the assembly interfaces, which are the interface regions of the large component to be joined to the final product. Before final assembly, the allowance is cleared so that the component fits to the whole aircraft within the tolerance requirements [3]. For example, Lei proposed a closed-loop machining system based on extended STEP-NC data models for the finishing machining of a vertical tail of a large passenger plane. The closed-loop machining system mainly consists of a three-axis machine tool, three CNC positioners, two laser trackers, and a holding device. Mathematic models for machining allowance evaluation, feature location, machining quality control of key features and final evaluation of machining quality were established according to the measurement data. Through real-time data feedback from two laser tracker and measuring probe, feature location modification machining parameters optimization can be realized and the final assembly quality of vertical tail improved significantly[1][4].

However, there are also many active components e.g. nose/main landing gear doors (NLGD/MLGD), cabin doors and etc which are assembled on the aircraft by using rotation shaft.

These components are usually assembled at the end of aircraft assembly. Meanwhile, because of the limitation of assembly operation space, assembly quality of these components are only guaranteed by the fabrication accuracy of components and improving assembly quality by means of finish machining is rarely studied. Furthermore, because the dimension of most aircraft doors are smaller relative to aircrafts, the influence on aerodynamic shape induced by their assembly quality is comparative smaller. As a matter of fact, the assembly quality optimization of aircraft doors is always not paid enough attention and performance of them are generally evaluated by the mechanic performance, such as working range, kinetic characteristics, etc. Nevertheless, for the military aircrafts especially the advanced ones have stealth and supersonic requirements, e.g. F22, F35, B2 and etc., which have even more strict demands for assembly quality of these active components, because the assembly defects like stepped difference, will lead to significant influence on not only aerodynamic performance, but also and importantly, stealth performance. Hence, improving the assembly quality of these large-scale active components to minimize the stepped difference is one of most crucial tasks for enhancing the final performances of aircraft, especially for military aircrafts.

To solve the problem, assembly quality optimization approach based on reverse engineering is one powerful and effective technique. Reverse engineering which is the process of obtaining a geometric CAD model from 3D measurements acquired by contact or non-contact scanning technique of an existing model[5][6][7]. Numbers of researches also have done in aircraft reverse engineering. Udroiu proposed a reverse engineering example of turbine blade, a Renishaw SP600 5-axis CMM with scanning probes was used to obtain the points cloud with high speed and high performance and the 3D model performed in the CATIA software[6]. This method can be used also for other complex parts from aircraft industry. Georgia Institute of Technology achieved the 3D model of the SR-71 Blackbird reconnaissance aircraft form the example. Aircraft aerodynamic, propulsive, or weights characteristics can be assessed and estimated using this 3D model [8]. Aiming to confirm the validity of the 6-DoF Aircraft Dynamics Model, a virtual sensor integrated in a low-cost navigation and guidance system designed for small Unmanned Aircraft (UA). Based on reverse engineering, Burston used the laser scanner and CATIA to re-construct the CAD model of AEROSONDE UA from published CAD model which was used in the calculation of the associated 6-DoF model parameters[9][10]. Jing re-constructed the 3D model of horizontal tail according to the points cloud collected by FARO TrackArm and laser tracker, the fabrication of the horizontal tail can be obtained correspondingly. The function of the laser tracker is to provide higher precise coordinates for reference points to achieve better registration accuracy [11]. However, these researches mainly focuses on approaches and methods to measure the difference between 3D modeling results and actual products, in other words, just using the reverse engineering as a tool to finish product inspection. But beyond that, reverse engineering is also employed in measurement-aided assembly. Reverse engineering was used to interface between the wing box ribs and the upper cover on the Advanced Low Cost Aircraft Structures (ALCAS) lateral wing box demonstrator. In this process measurements of the cover profile were used to generate machining paths for the fettling of rib feet. The rib feet were then machined using a standard 6-axis industrial robot mounted on a gantry over the wing box robot [12]. Nonetheless, because the assembly form and sequence of active component, optimizing assembly quality just through shimming and fettling are generally hard to realize. Meanwhile, the limit of operation space enable the way of finishing machining is difficult to achieve.

Aiming to improve the assembly quality and overcome the shortages of current researches, this paper proposes an assembly quality optimization approach for aircraft doors based on reverse engineering. Section 2 discusses main inducements of active components assembly quality problem. Afterwards, reverse engineering using laser scanner is introduced in Section 3. In Section 4, Assembly quality optimization model based on measurement data is proposed and analyzed. A case study in Section 5 aims to verify the proposed method and mathematical model. Finally, conclusion and discussion are given.

2. Inducements of active components assembly quality problem

The assembly of large aerospace structures is characterized by a reliance on monolithic jigs and high levels of manually intensive reworking, fettling and drilling operations. In simple terms the

process is to bring together large flexible components and secure them to a rigid jig which controls the shape of the emerging structure [13]. Here, MLGD is taken as a typical example to illustrate the inducements of assembly quality problem. Fabrication error, assembly error and deformation of active components will induce assembly quality problem such as interference, gap and stepped difference.

2.1 Fabrication workflow of MLGD

The MLGD is a non-load-bearing structure of aircraft. With lightweight requirement of modern aircraft, the MLGD generally is made of composite material [14]. Figure1 demonstrates the brief workflow of MLGD, which mainly includes following five steps,

Cementing outer skin, ribs and trusses together, and then curing in autoclave system. In this step, positioning jig is adopted to guarantee the relative posture of each components.

Assembling corner fillets. The function of corner fillet is to intensify joint reliability between ribs and trusses. Because corner fillets are only employed to connect ribs and trusses, assembly accuracy requirement is less demanding.

Assembling beams. Beams whose material often adopt aluminum alloy or titanium alloy, are main support structure of MLGD. Meanwhile, postures of beams, ribs and trusses determine the relative posture relationship between inner skin and outer skin.

Intersection holes which are used to connect MLGD and frame are drilled with the help of assembly jigs. The spatial direction of intersection hole will determine the relative posture relationship between MLGD and frame.

Cementing the inner skin. In this step, assembly jigs are adopted to position postures of components and control the shape of the emerging MLGD. Finally, shimming and fettling are executed by means of inspection jigs to fit the theoretical model of MLGD.

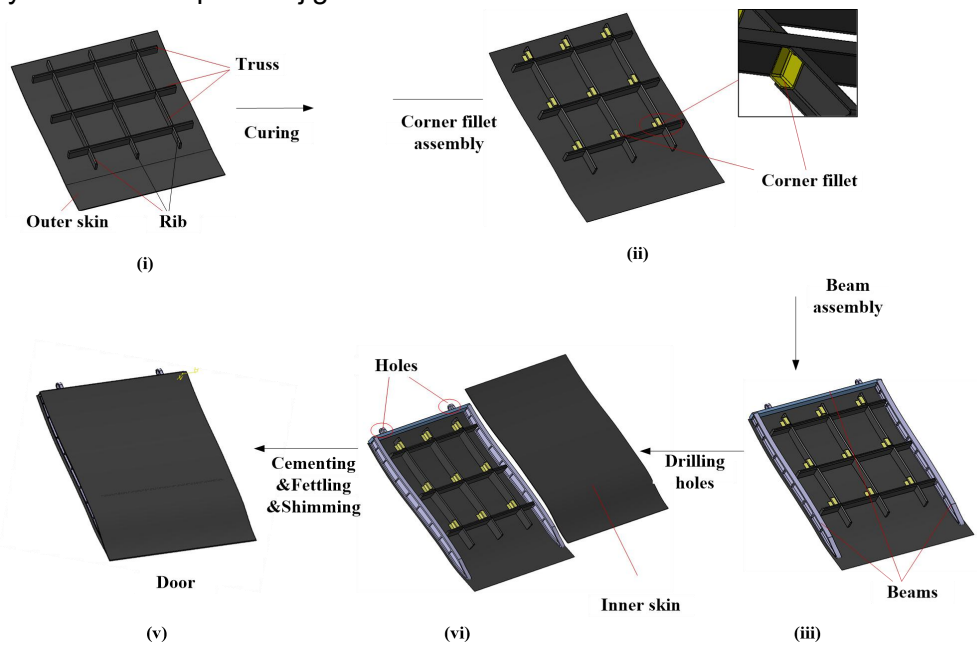

Figure 1 Fabrication workflow of main landing gear door

2.2 Assembly workflow of MLGD

The frame has been assembled on the fuselage with help of assembly jigs before MLGB assembly. Generally, the frame is made of aluminum alloy or titanium alloy, and features of frame, i.e. shape, holes, etc., can be machined by high-precision NC machine tool. However, there are still non-negligible difference between as-built model and theoretical model due to machining error, assembly error delivery error and fabrication error of jigs. Then, as Figure2 (a) shown, the door and the frame are connected together by a shaft. After assembly, the door can rotate around the axis within a certain angle range. In the assembly process, assuring the coaxiality of intersection holes is the primary task and the stepped differences, interferences and gaps between MLGD and frame will inevitably appear due to fabrication error, assembly error and deformation, as shown in Figure2(b).

Different from traditional assembly workflow, the aircraft door assembly is at the end of the whole assembly process and there is not enough volume to drill the holes of the door in-jig, therefore the intersection holes on the active components and the frames are drilled according to machining jigs before assembly respectively. Automatic finishing machining in-jig to optimize the assembly quality is always not allowed due to the operation volume limit.

Generally, as-built dimension of MLGD often smaller than as-design model, interference can be avoid correspondingly. And then, with regard to the gaps, concealed edge band which is made of elastic material is often used in modern military aircraft, e.g. F35 and F22, and have achieved good application result. However, while as for the stepped difference, there is no effective method. Taking fabrication error, assembly error and deformation into account, the inducements of MLGD assembly problem can be illustrated in Figure3.

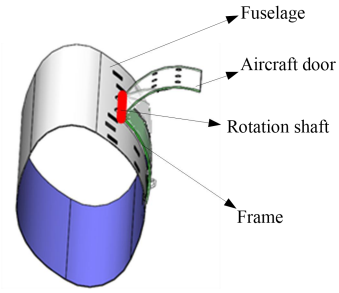

(a) Aircraft door state after assembly

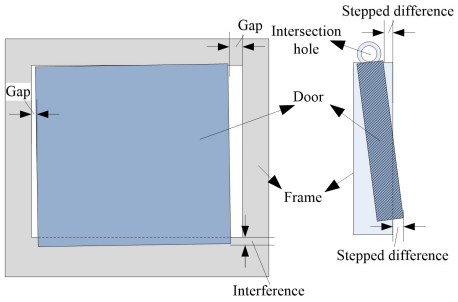

(b) Step difference in aircraft door assembly

Figure 2 Diagram of typical Aircraft active component assembly

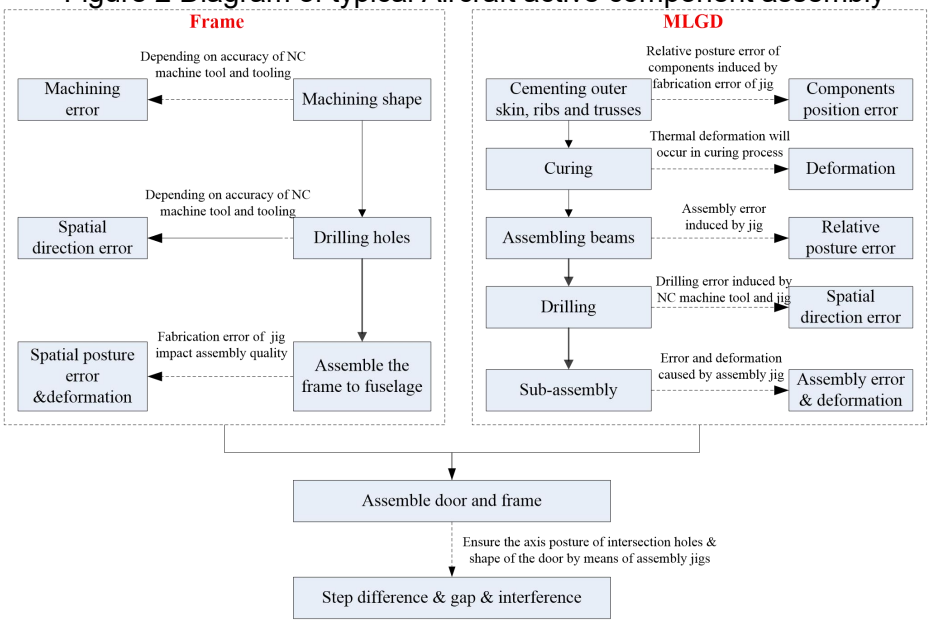

Figure 3 Roots of assembly quality problem

Above all, the aircraft door assembly is at the end of the whole assembly process of the aircraft and have two challenges. On one hand, issues related to maintaining high tolerances are the biggest challenges; the doors are flexible components and interfaces of them are often imprecise because they are usually made of composite materials in order to reduce weight; and it is very difficult to drill intersection holes with high precision in doors and frame respectively which will match and lock the assembly into its correct overall form because of the operation space limit. The current solution is to drill the intersection holes in doors and frame with the help of coordinate jigs when they are in part state and use a monolithic jig which holds door to its correct final form as the assembly is built-up, employ the intersection holes to link the door and frame. This process results in additional process steps, inflexibility due to reliance on monolithic jigs and inefficient craft based production due to high levels of reworking in-jig. What is more, because of the influence of drilling error of intersection holes, fabrication error of door, the coordination error the assembly jigs, sub-assembly error of frame and etc., stepped difference will appear inevitably. As Figure4 shown, the stepped difference cannot eliminate through the fettling and shimming, because these process can

impact the strength of the door. However, it is too expensive even not practical to optimize the stepped difference if only by means of minimizing the errors of aforementioned impact factors. Therefore, using the measurement data of the door and the frame based on reverse engineering to computing the optimal axis of intersection holes of the door which leads to the minimum stepped difference seems like a promising way to optimize the assembly stepped difference.

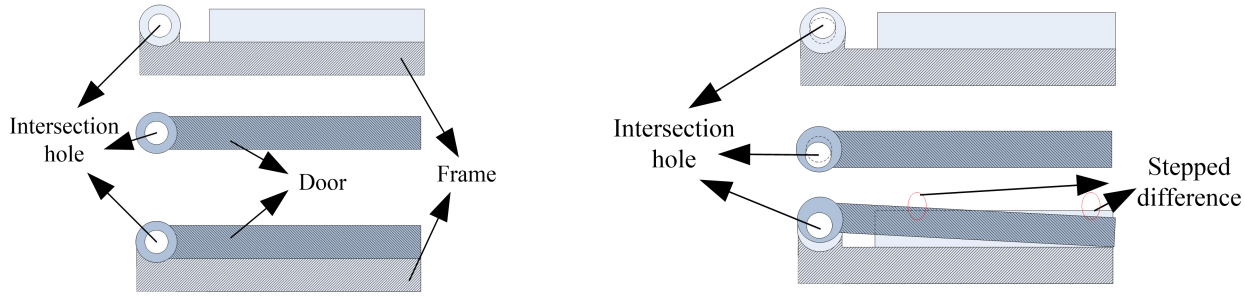

(a) Ideal assembly state (b) Actual assembly state

Figure 4 Common assembly problems in aircraft door assembly

3. Measurement data acquisition using laser scanner

3.1 Laser scanner description

Different laser 3D scanners have the similar structure and working principle. The combination of Dual-camera vision system and laser ranging system can realize object position and surface topography. Two cameras with intersecting optical axes shoot the same object from different angles to obtain the geometric mapping between the camera and the object. The laser ranging system composed of laser generator and CCD obtains the coordinates of surface points based on the triangulation principle. Combination of photography and laser scanning has both the technical advantage of photography reference point and the high-speed advantage of laser scanning.

3.2 Principle of three-dimensional reconstruction

Internal and external parameters of the camera should be calibrated before scanning, such as the rotation and translation matrix between the two cameras. During the scanning operation, multiple mark points appear simultaneously in the double cameras, and it is necessary to match the image points of the same name to determine the corresponding relationship of the image points in the double cameras. Based on the imaging principle and transformation matrix of double cameras, image points with the same name can be recognized according to geometric relations among image points, object points and projection centers.

The geometric mapping relation between the camera and the target basically depends on the mark points. As Figure5 shows, the dual camera system takes the mark points from different fields of view at the same time, and calculates the three-dimensional coordinate value according to the parallax of the mark points in the two images.

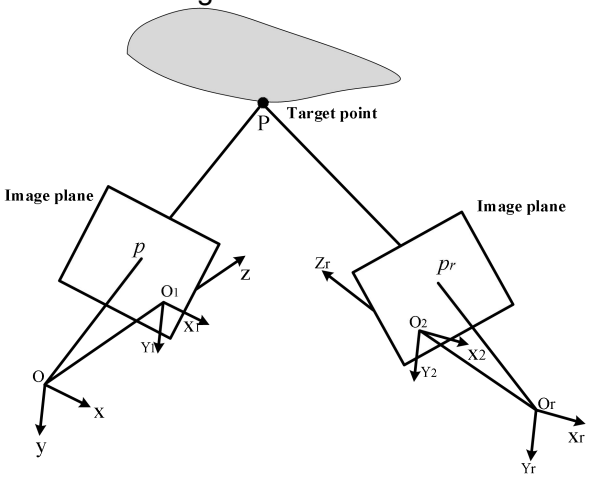

Figure 5 Nephogram of morphology deviation

Mark point P on the surface of the part is denoted as p and pr on the corresponding imaging plane of the dual camera system. The coordinate of P in coordinate system O-xyz is (X, Y, Z), the

coordinate of p in coordinate system o-xyz is (x, y, -f1).The coordinate of pr in coordinate system Or-$x_ry_rz_r$ is (x_r, y_r, -f_r), the coordinate of P in coordinate system O-$x_ry_rz_r$ is (X', Y', Z'). In the dual camera system, the formula (1) and (2) can be derived from the collinear relationship between the object point, the image point and the coordinate origin.

$$\begin{cases} \dfrac{x}{X} = \dfrac{y}{Y} = \dfrac{z}{Z} \\ \dfrac{x_r}{X'} = \dfrac{y_r}{Y'} = \dfrac{z_r}{Z'} \end{cases} \tag{1}$$

Since the relative position between the two cameras of laser scanner has been calibrated, the mutual positional relationship between O-xyz and Or-xryrzr can be represented by a fixed rotation matrix R and a translation matrix T. Relationship between (X, Y, Z) and (X', Y', Z') can be represented by formula (1). Coordinate of point P in O-xyz can be solved according to,

$$\begin{bmatrix} X \\ Y \\ Z \end{bmatrix} = R \begin{bmatrix} X' - T_x \\ Y' - T_y \\ Z' - T_z \end{bmatrix} \tag{2}$$

When the mark points of the known coordinate values are detected during the scanning process, the current location and pose of the camera can be solved according to the points. If a new mark point is acquired in the field of view, the new mark point would be added to the global coordinate system. Then, all the mark points constitute the control network of the system, as shown in Figure6.

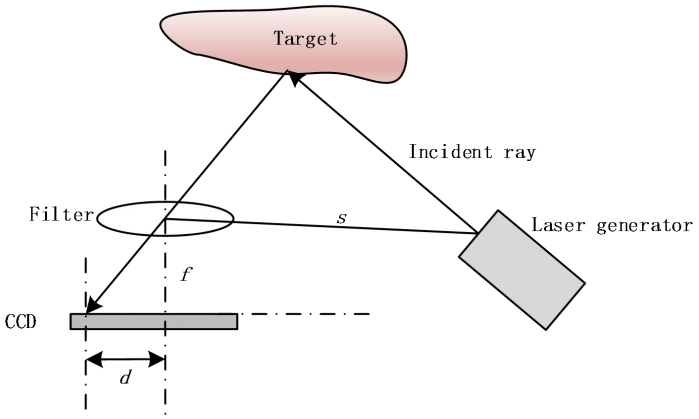

Figure 6 Principle of triangle measurement

Under the precise coordinate network formed by mark points, the distance between scanner and object is calculated based on laser triangulation method. Since the mapping relationship between scanner and the object has been solved by the dual-camera positioning principle, the coordinates of the surface topography point cloud in the global coordinate system can be solved by matrix transformation.

4. Assembly quality optimization model based on measurement data

After as-built models of frame and MLGD achieved by means of 3D reconstruction, assembly quality optimization mathematical model can be established. Because of gaps and interference can be eliminated by means of concealed edge band, objective of assembly quality optimization is to minimizing the stepped difference in this paper. According to section 2, the objective of stepped difference optimization is to compute the best axis of the MLGD intersection hole which can be calculated by the workflow in Figure7.

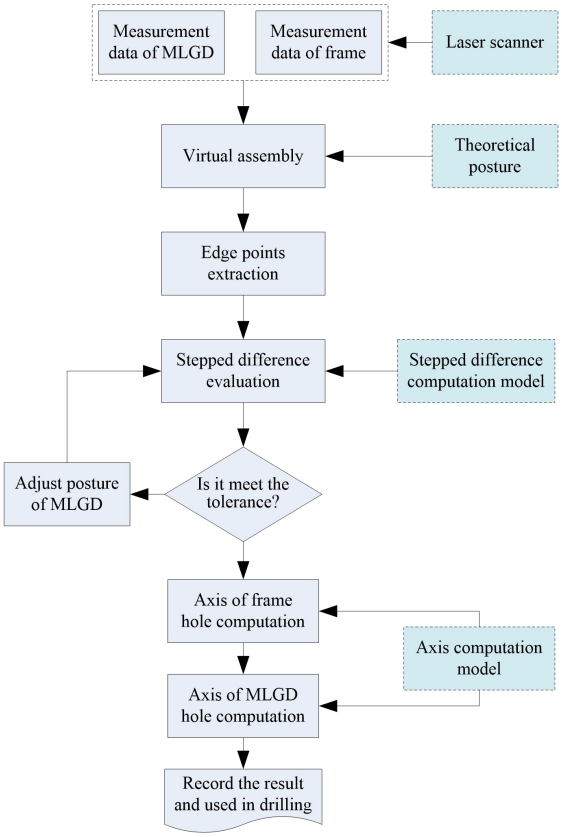

Figure 7 Intersection hole axis best fit workflow for the MLGD

The main computation workflow can be denoted as following 4 steps,

(i) Virtual assembly. After models of MLGD and frame are reconstructed based on measurement data, the frame and the MLGD can be virtually assembled together. In the design assembly, the posture of MLGD relative to the frame can be expressed by rotation matrix RI and translation matrix TI in initial state,

$$R_I = \begin{bmatrix} \cos\gamma_I \cos\beta_I & \cos\gamma_I \sin\beta_I \sin\alpha_I - \sin\gamma_I \cos\alpha_I & \cos\gamma_I \sin\beta_I \cos\alpha_I + \sin\gamma_I \sin\alpha_I \\ \sin\gamma_I \cos\beta_I & \sin\gamma_I \sin\beta_I \sin\alpha_I + \cos\gamma_I \cos\alpha_I & \sin\gamma_I \sin\beta_I \cos\alpha_I - \cos\gamma_I \sin\alpha_I \\ -\sin\beta_I & \cos\beta_I \sin\alpha_I & \cos\beta_I \cos\alpha_I \end{bmatrix} \tag{3}$$

$$T_I = \begin{bmatrix} T_{Ix} & T_{Iy} & T_{Iz} \end{bmatrix}^T \tag{4}$$

where, $(\alpha I, \beta I, \gamma I)$ are Euler angles to describe rotation value of MLGD and $(T_{Ix}, T_{Iy}, T_{Iz}]$ denote the position of the MLGD.

(ii) Stepped difference evaluation. According to measurement data, measured points of MLGD and frame are written as,

$$\mathbf{P_D} = \{P_{Di}, i = 1,2,\cdots m\} \tag{5}$$

$$\mathbf{P_F} = \{P_{Fi}, i = 1,2,\cdots n\} \tag{6}$$

For a profile of interface between MLGD and frame, the edge points of them can be extracted from the P_D and P_F and written as P_{DE} and P_{FE} respectively, as Figure8 shows. The stepped difference can be denoted as

$$h = \max\{h_i\} \tag{7}$$

where, h_i is distance from P_{Di} to line AB. The line AB can be expressed by following formula and fitted based on edge points of frame,

$$\frac{x - x_0}{l} = \frac{y - y_0}{m} = \frac{z - z_0}{n} \tag{8}$$

$$h_i = \frac{\sqrt{\left[m(z_{FEi} - z_0) - n(y_{FEi} - y_0)\right]^2 + \left[n(x_{FEi} - x_0) - l(z_{FEi} - z_0)\right]^2 + \left[l(y_{FEi} - y_0) - m(x_{FEi} - x_0)\right]^2}}{\sqrt{l^2 + m^2 + n^2}} \tag{9}$$

where, $[l, m, n]$ is the direction vector of axis of the MLGD intersection hole, $[x_0, y_0, z_0]$ is a random

point at line AB.

Assembly interface can be divided into numbers of regions and the maximum value of stepped difference is

$$H = \max\{h\} \tag{10}$$

Compared with tolerance, H can be used to evaluate whether the assembly meet the assembly quality requirement.

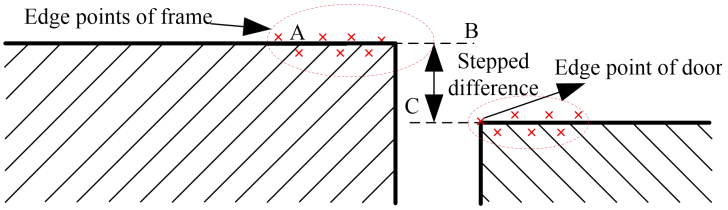

Figure 8 Stepped difference between frame and MLGD in a profile

(iii)Best axis computation. If the stepped difference exceed the tolerance requirement, optimization should be executed. A variation which can be expressed by [$\triangle\alpha_I$, $\Delta\beta_I$, $\Delta\gamma_I$, ΔT_{Ix}, ΔTIy, • ΔT_{Iz}] can be added to [α_I, β_I, γ_I, T_{Ix}, T_{Iy}, T_{Iz}]. According to formula (3) and (4), the rotation and translation matrices can be reset as,

$$R_i = \begin{bmatrix} \cos\gamma_i\cos\beta_i & \cos\gamma_i\sin\beta_i\sin\alpha_i - \sin\gamma_i\cos\alpha_i & \cos\gamma_i\sin\beta_i\cos\alpha_i + \sin\gamma_i\sin\alpha_i \\ \sin\gamma_i\cos\beta_i & \sin\gamma_i\sin\beta_I\sin\alpha_i + \cos\gamma_i\cos\alpha_i & \sin\gamma_i\sin\beta_i\cos\alpha_i - \cos\gamma_i\sin\alpha_i \\ -\sin\beta_i & \cos\beta_i\sin\alpha_i & \cos\beta_i\cos\alpha_i \end{bmatrix} \tag{11}$$

$$T_i = \begin{bmatrix} T_{ix} & T_{iy} & T_{iz} \end{bmatrix}^T \tag{12}$$

$$\begin{cases} \alpha_i = \alpha_I + \Delta\alpha_I \\ \beta_i = \beta_I + \Delta\beta_I \\ \gamma_i = \gamma_I + \Delta\gamma_I \\ T_{ix} = T_{Ix} + \Delta T_{Ix} \\ T_{iy} = T_{Iy} + \Delta T_{Iy} \\ T_{iz} = T_{Iz} + \Delta T_{Iz} \end{cases} \tag{13}$$

In this optimization process, following restriction should be satisfied, i.e. there is interference between frame and MLGD,

$$P_D \notin P_F \tag{14}$$

Then, the stepped difference can be evaluated again by step (ii) until meeting the assembly quality requirement. The optimization value of parameter is [$\Delta\alpha$, $\Delta\beta$, $\Delta\gamma$, ΔTx, ΔTy, ΔTz].

(iv)Rotation axis fit. As shown in Figure9, the axis of the MLGD intersection hole can be fitted according to measurement data. The axis of intersection hole can be denoted as,

$$\frac{x - x_{D0}}{l_D} = \frac{y - y_{D0}}{m_D} = \frac{z - z_{D0}}{n_D} \tag{15}$$

where, [l_D, m_D, n_D] is the direction vector of axis of the MLGD intersection hole, [x_{D0}, y_{D0}, z_{D0}] is a random point at axis.

The distance from measured points P_i to axis is,

$$d = \frac{\sqrt{\left[m_D(z_i - z_{D0}) - n_D(y_i - y_{D0})\right]^2 + \left[n_D(x_i - x_{D0}) - l_D(z_i - z_{D0})\right]^2 + \left[l_D(y_i - y_{D0}) - m_D(x_i - x_{D0})\right]^2}}{\sqrt{l_D^2 + m_D^2 + n_D^2}} \tag{16}$$

where, (x_i, y_i, z_i,) is 3D coordinates of Pi, when Pi is on outer-surface of the hole, the value of d is router, and when Pi is on inner-surface of the hole, the value of d is r_{inner}. Take measurement error, fabrication error and other errors into consideration, the formula(4) should be written as,

$$\frac{\sqrt{\left[m_D(z_i - z_{D0}) - n_D(y_i - y_{D0})\right]^2 + \left[n_D(x_i - x_{D0}) - l_D(z_i - z_{D0})\right]^2 + \left[l_D(y_i - y_{D0}) - m_D(x_i - x_{D0})\right]^2}}{\sqrt{l_D^2 + m_D^2 + n_D^2}} - d = \varepsilon_i \tag{17}$$

where, ε_i is the fit error. The parameters [l_D, m_D, n_D, x_{D0}, y_{D0}, z_{D0}] can be obtained by solving the formula (5) with support of no less than 6 measured points. Similarly, the axis of the frame intersection hole whose corresponding parameters are [l_F, m_F, n_F, x_{F0}, y_{F0}, z_{F0}] can be computed and

expressed as,

$$\frac{x-x_{F0}}{l_F}=\frac{y-y_{F0}}{m_F}=\frac{z-z_{F0}}{n_F} \tag{18}$$

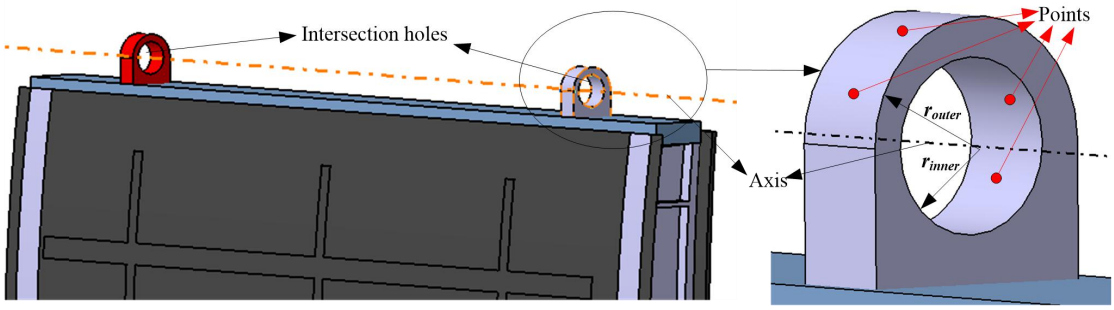

Figure 9 Rotation axis fit

According to the result of step (iii) and formula (17), in order to obtain the optimal assembly posture of MLGD, the posture of MLGD can be adjusted to [αI+Δα, βI+Δβ, γI+Δγ, TIx+ΔTx, TIy+ΔTy, TIz+ΔTz].

5. Experiment and verification

5.1 Overview of the study case and experimental setup

In this section, simulated specimens of MLGD (Figure10(a)) and frame (Figure10(b)) which is made of aluminum alloy as shown in Figure 10 is used as a study case. Random error is added in order to simulate fabrication error of MLGD. The tolerance of stepped difference is from -0.3mm to 0.3mm.

A HanyScan 700 elite laser scanner provided by Creaform Co. Ltd is employed to acquire the measurement data of the MLGD and the frame. Ø6mm mark points are sticked on surface of simulator equally to image stitching, as Figure11 shown. By means measurement and 3D reconstruction, measurement models of MLGD and frame can be obtained, which are shown in Figure12. Based on workflow of section 4, as Figure13, the interface is divided into 400 regions. The stepped difference can be computed by computation mathematical model. It can be seen in Figure14, stepped differences of about 77 regions exceed tolerance, and in other words, the assembly quality of MLGD cannot meet the assembly requirement.

Therefore, the axis of the MLGD should be optimized based on workflow of Figure7. The optimization parameters are shown in Table 1. Based on these parameters, the axis of intersection can be amended and the stepped difference optimization can be achieved. Figure15 signifies that stepped differences of all regions are within assembly tolerance requirement.

(a) MLGB simulator (b) MLGB simulator

Figure 10 Simulators of study case

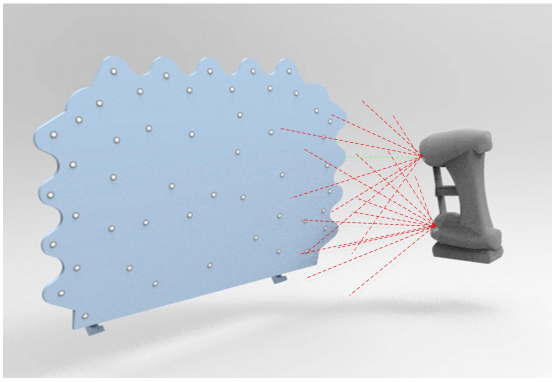

(a) MLGB measurement

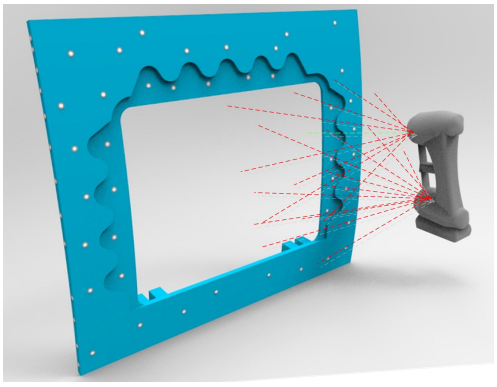

(b) MLGB measurement

Figure 11 Measurement process of simulators

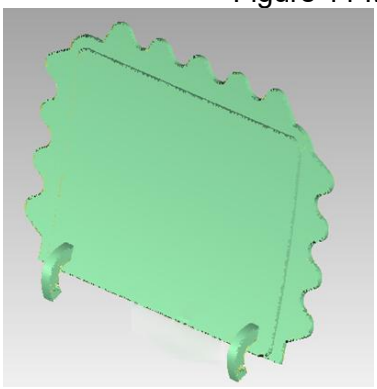

(a) MLGB measurement model

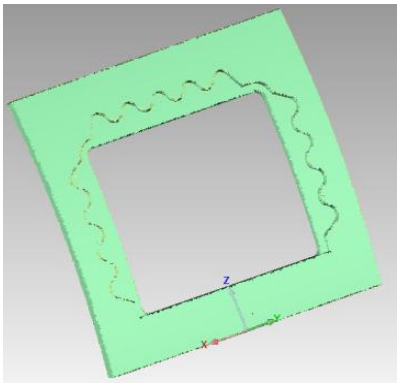

(b) MLGB measurement model

Figure 12 Measurement models of simulators

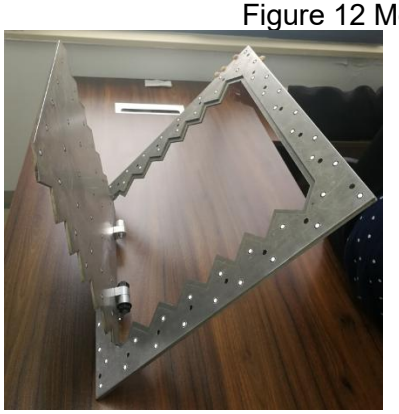

(a) MLGB assembly

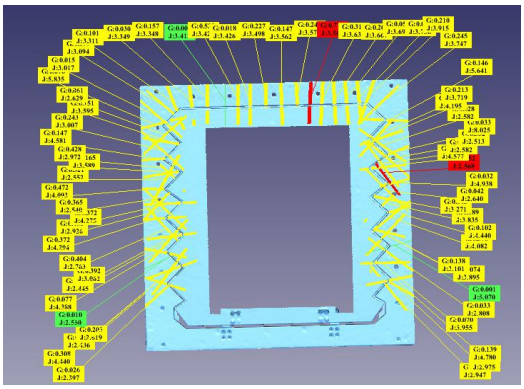

(b) Stepped difference evaluation

Figure 13 Stepped difference evaluation in theoretical state

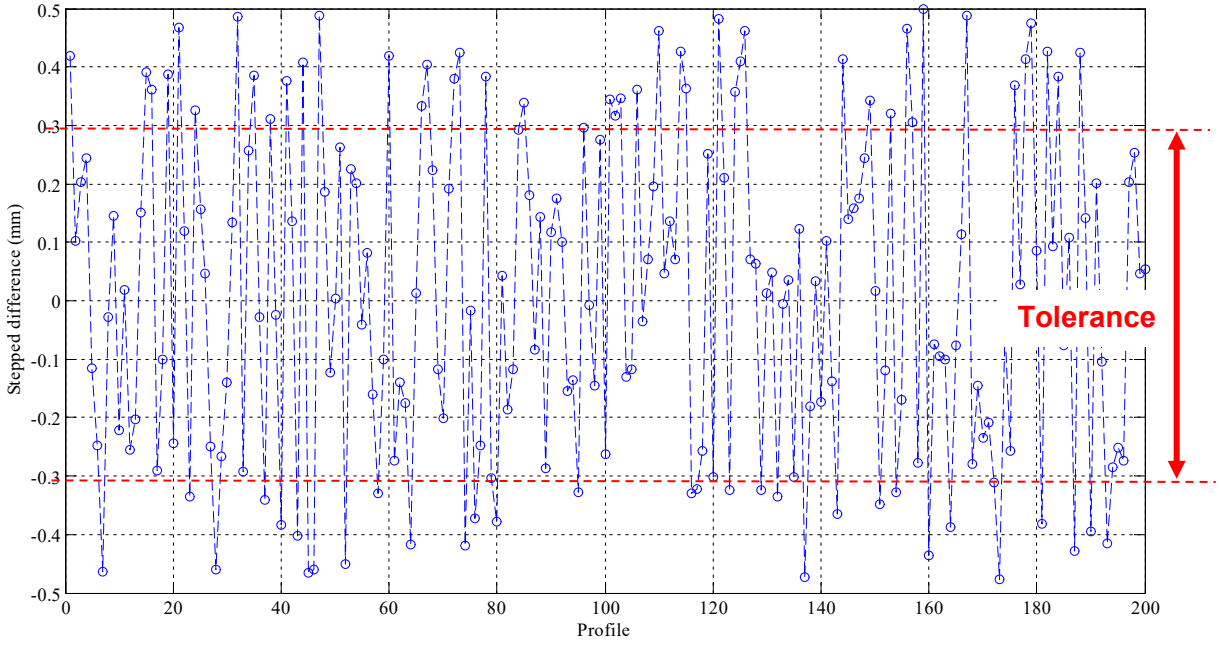

Figure 14 Stepped difference before optimization

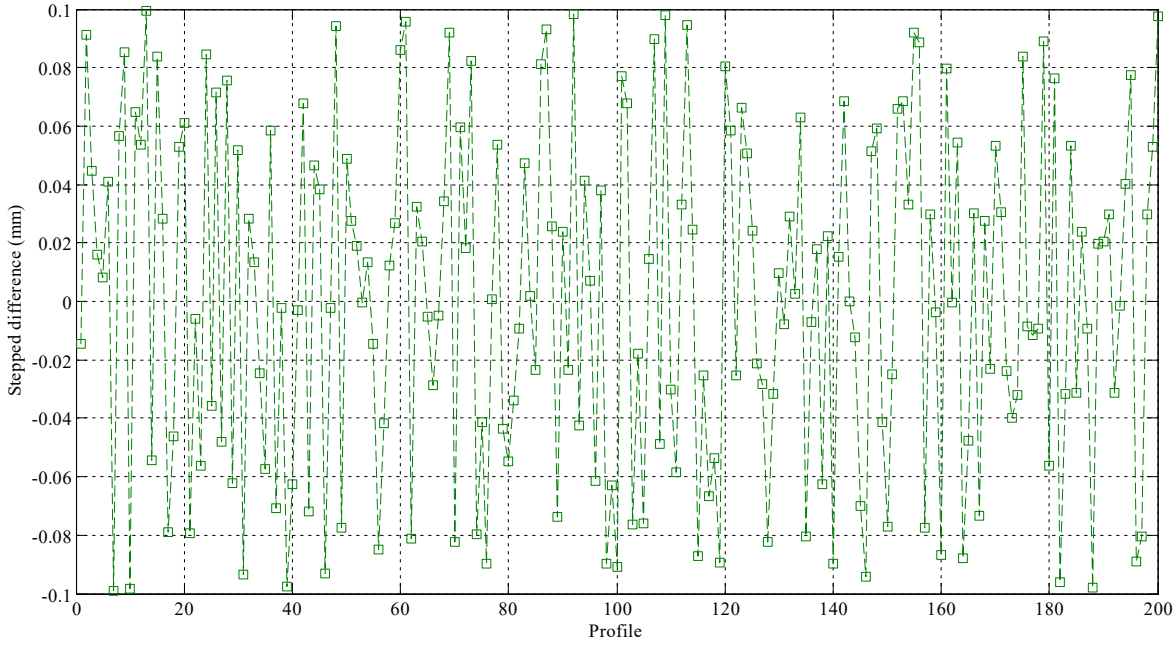

Figure 15 Stepped difference after optimization

Table 1 Optimization parameters

△α (arc)	△β (arc)	△γ(arc)	△ Tx (mm)	△ Ty (mm)	△ Tz (mm)
0.0231	0.0051	0.0010	0.3081	0.5122	0.3321

6. Conclusion and discussion

In order to optimize assembly quality of aircraft active components, assembly quality optimization for active components of aircraft based on reverse engineering is proposed in this paper. Assembly problems existed in large-scale active components assembly, i.e. gap, interference and stepped difference, are discussed firstly. The assembly errors mainly source from fabrication error and assembly error. However, this paper just focuses on the stepped difference, but not pays more attention to gap and interference due to they can optimized by using concealed edge band.

Reverse engineering based on laser scanner which is a much powerful method to collect measurement data is introduced. Only one deficiency of this system is that image stitching error will accumulates although marker points are used to improve the accuracy. With the development

of digital measurement systems, hybrid measurement system increasingly become the future trend. For marker used to image stitching, high-precision calibration used coordinate measuring machine (CMM), closed-range photgrammetry or other ultra-precision system, will further upgrade the measurement accuracy.

Furthermore, the stepped difference evaluation mathematical model seems like a method of exhaustion. It will cost waste of computation time and efficiency. Therefore, a future work which aims to improve optimization efficiency by means some advance algorithm, like particle swarm optimization (PSO), genetic algorithm and etc. should be researched.

Despite these shortcomings, the presented mathematic model can still offer scientific and systematic method and guideline for assembly quality optimization of active components. The example of measurement scenario demonstrates that the proposed method is feasible and effective and will lay a foundation for active component assembly quality improvement.

References

[1] Lei P, Zheng L Y, Xiao W L, et al. A closed-loop machining system for assembly interfaces of large-scale component based on extended STEP-NC [J]. Int J Adv Manuf Technol, 2017, (6):

[2] Muelaner JE, Kayani A, Martin O, Maropoulos P (2011) Measurement Assisted Assembly and the Roadmap to Part-To-Part Assembly [C]. In: 7th International Conference on Digital Enterprise Technology, University of Bath, pp 11–19

[3] Maropoulos PG, Muelaner JE, Summers MD, Martin OC (2013) A new paradigm in large-scale assembly:research priorities in measurement assisted assembly [J]. The International Journal of Advanced Manufacturing Technology 70(1–4):621–633.

[4] Lei P, Zheng L Y. Closed-loop calibration method of PPPS mechanism ball joint center position for posture adjustment of large aircraft components [J]. Acta Aeronautica et Astronautica Sinica, 2016, 37(10):3186-3196.

[5] Chen L C, Lin G C I. A vision-aided reverse engineering approach to reconstructing free-form surface [J]. Computer integrated manufacturing systems, 1997, 10(1): 49-60.

[6] Udroiu R. Research regarding reverse engineering for aircraft components [C]. MATEC Web of Conference 94, 01012, 2017.

[7] Cioana C, Tulcan A, Grozav I. Scanning straegies for aluminium and plastic parts [J]. Solid state phenomena, 2012, 188: 406-411.

[8] German B. A case study approach to teaching aircraft performance: reverse engineering the SR-71 blackbird [R], American Society for Engineering Education, AC-2010-2161.

[9] Burston M.T., Sabatini R., Clothier R., et al. Reverse engineering of a fixed wing unmanned aircraft 6-dof model for navigation and guidance applications [J]. Applied Mechanics and Materials, 2014, 629 :164-169.

[10] Sabatini R., Ramasamy S., Gardi A., et al. Low-cost Sensors Data Fusion for Small Size Unmanned Aerial Vehicles Navigation and Guidance [J]. International Journal of Unmanned Systems Engineering, 2013, 1(3): 16-47.

[11] Jing X.S., Zhang P.F., Wang Z.J., et al. Digital combined measuring technology assisted quality inspection for aircraft assembly [J]. Journal of Beihang University, 2015, 41(7): 1196-1201.

[12] Maropoulos P.G., Muelaner J.E., Summers M.D. A new paradigm in large-scale assembly–research priorities in measurement assisted assembly [J]. International Journal of Advanced Manufacturing Technology, 2014, 70 (1–4): 621–633.

[13] Muelaner J, Maropoulos P G. Large scale metrology in aerospace assembly [C]. Proceedings of DET2008 5th International Conference on Digital Enterprise Technology Nantes, France, 22-24 October 2008

[14] Fan Y.Q., Mei Z.Y., Tao J. Large aircraft digital manufacturing engineering [M]. Beijing: Aviation industry press, 2011.

7. Contact Author Email Address

Corresponding Author Email Address: zhuxusheng@buaa.edu.cn

8. Copyright Statement